

N DOPING: PROGRESS IN DEVELOPMENT AND UNDERSTANDING*

A. Grassellino, A. Romanenko, S Posen, Y. Trenikhina, O. Melnychuk, D.A. Sergatskov, M. Merio,
Fermilab, Batavia, IL 60510, USA

M. Checchin, M. Martinello, Fermilab and Illinois Institute of Technology,
Chicago, IL 60616, USA

Abstract

Following the 2012 discovery at Fermilab of a systematic increase of the quality factor of SRF bulk niobium cavities via nitrogen doping of the RF surface, Fermilab has moved forward with the development of this new technology, expanding from single cell to multicell cavities and to cavities of different frequencies. Extensive effort has been dedicated to the understanding of the underlying phenomena leading to the improved performance. This contribution will summarize the recent state of the art development and understanding of the N doping technology at FNAL.

INTRODUCTION

N doping was discovered in 2012 at FNAL and proven to systematically raise Q factors in the mid accelerating field region $B_{pk} > 60$ mT. In particular, N doping is found to lower the BCS surface resistance compared to 120C baked and unbaked niobium by a factor of ~ 2 at fields > 60 mT, and to lower non trapped flux related residual resistance < 2 n Ω [1]. Following the discovery on single cells, FNAL worked on: a) understanding the parameters in play leading to the improved performance; b) searching for the optimal doping recipe leading to best performance, in particular for Q, quench fields and trapped flux induced losses; c) develop quickly the technology on 1.3 GHz nine cells for LCLS-2 [2,3]; d) study cavity cutout and flat samples with various surface techniques looking for correlation with performance [4]; and e) apply the findings to 650 MHz cavities. A timeline summarizing the N doping R&D at FNAL is shown in Fig. 1.

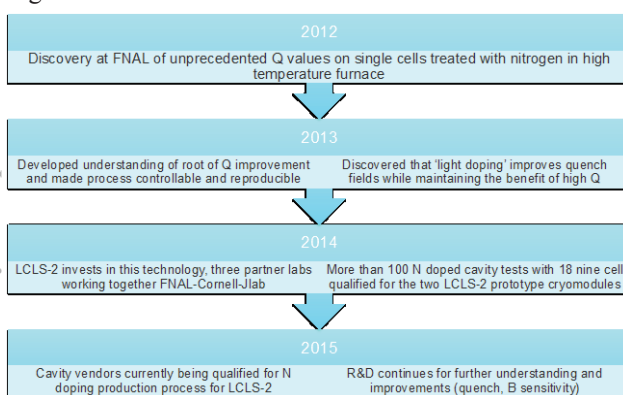


Figure 1: Timeline summarizing the development of the N doping technology from the 2012 discovery to today.

*Work supported.
#cee@aps.anl.gov

PROGRESS IN N DOPING DEVELOPMENT: LCLS-2 AND PIP-2

A variety of doping bake regimes have been explored at FNAL for single and multicell cavities of different frequencies 1.3 GHz and 650 MHz, in the context of development of a baseline surface treatment protocol for the LCLS-2 [5] and PIP-2 projects [6]. In both cases Q maximization at medium accelerating gradients ~ 17 MV/m and operating temperatures of ~ 2 K is desired for minimization of cryogenic costs. Figure 2 shows the so far optimal recipe found and currently adopted as LCLS-2 baseline cavity surface processing protocol, the recipe known as "2/6" which stands for 2 minutes nitrogen injection, 6 minutes anneal, all at 800C, followed by 5 microns electro polishing average surface removal [7]. As it can be seen from Fig. 2 the processing sequence is a small variation from the standard protocol for example adopted by XFEL, involving small changes during the furnace treatment, the post furnace EP, and the removal of the final 120C bake. The 120C bake does not bring performance benefit to N doped surfaces, actually a decrease in Q and quench fields has been observed to N doped cavities that have been also 120C baked.

Example from a doping process developed for LCLS-2

- Bulk EP
- 800 C anneal for 3 hours in vacuum
- 2 minutes @ 800C nitrogen diffusion
- 800 C for 6 minutes in vacuum
- Vacuum cooling
- 5 microns EP

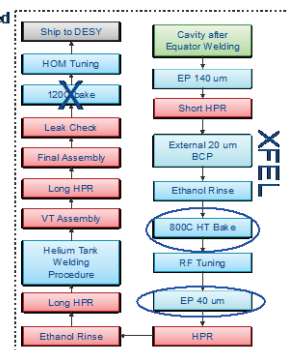
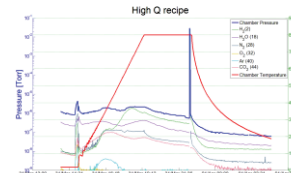


Figure 2: Example of doping protocol, small variation from the standard surface processing sequence.

The development of N doping for LCLS-2 is extensively described in [2,3]. Figure 3 shows one of the milestone plots which is the vertical test qualification of the nine cell cavities, treated with the 2/6 recipe, for the two LCLS-2 prototype cryomodules. All cavities meet the specification of 2.7×10^{10} at 2K, 16 MV/m, and a record average quality factor is achieved of $\sim 3.5 \times 10^{10}$ at 2 K, 16 MV/m. The bottom plot shows the same recipe applied to 650 MHz cavities, compared to standard 120C bake processing. Also in this case a gain up to a factor of 2 in quality factor at mid-field is found, and a record Q of $\sim 7 \times 10^{10}$ at 16 MV/m, 2 K is reached.

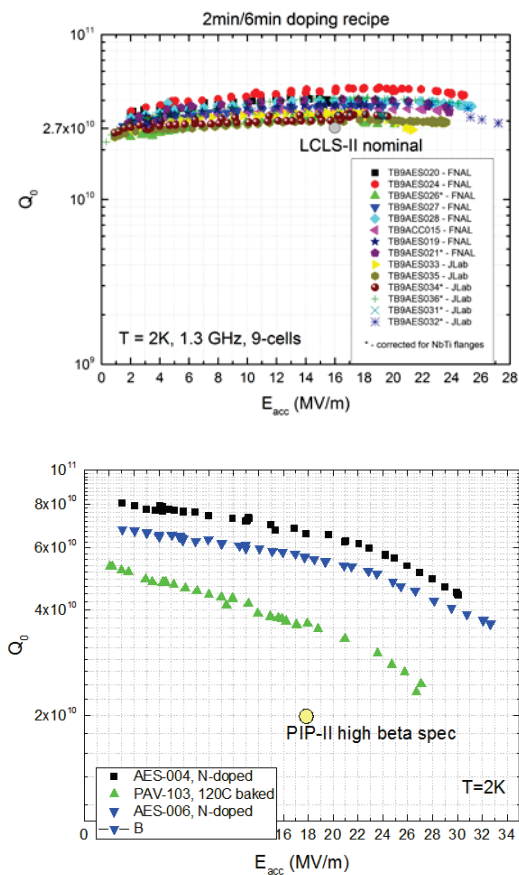


Figure 3 top: LCLS-2 nine cell cavities performance and bottom: 650 MHz cavities performance for 2/6 N doping recipe vs 120C bake standard treatment.

PROGRESS IN UNDERSTANDING

N doping discovery followed studies aimed at creating a niobium nitride layer by reacting the cavity with nitrogen at high temperature. The quality factors obtained right after furnace treatment and pre-EP were always low $\sim 1e7 - 1e8$, indicating formation of poorly SC Nb N phases. The improvement was always found post furnace treatment plus some amount of EP removal. At that point two scenarios were possible to explain the origin of the Q improvement: 1) niobium nitride forming in layers, outer ones poorly SC and inner ones of the right composition to give NbN with Tc higher than Nb; 2) residual nitrogen left as interstitial modifying the mean free path and/or the SC gap beneficially compared to ‘undoped’ niobium. Extensive samples studies were then performed to investigate these two different scenarios. Figure 4 (top) shows SEM images of samples post furnace treatment with nitrogen for different recipes (2/6 and 20/30) showing clear formation of nitride precipitates. The size of the precipitates is clearly larger for the 20 minutes injection/ 30 minutes anneal recipe. On the bottom left of Fig. 4 a SEM cross section of the 2/6 treated sample shows that the discrete NbN precipitates penetrate the surface at a depth ~ 0.2 microns in the shape of what

looks like a sharp protrusion. Diffraction patterns of transmitted electrons confirm that the sharp protrusions are poor phases of NbN as it can be seen in the bottom right image of Fig. 4.

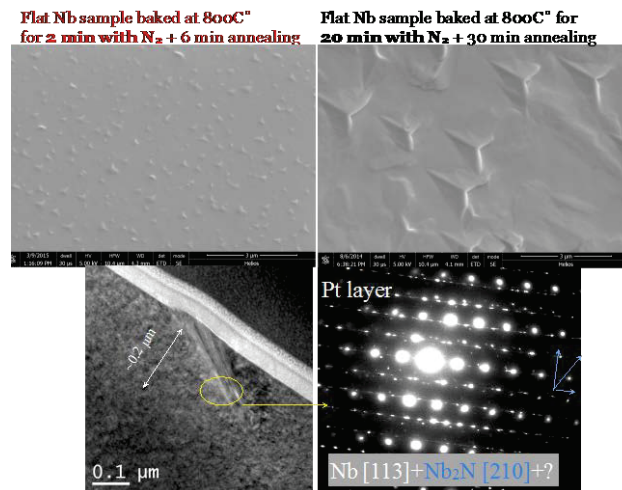


Figure 4 top: LCLS-2 nine cell cavities performance.

Figure 5 shows as a comparison the diffraction pattern for the same sample as Fig. 4, but post 5 microns EP. This is representative of the surface treatment of cavities showing the best performance with the 2/6 plus 5 microns protocol. As it can be seen the diffraction pattern now shows only clean niobium and no nitride phases, indicating that the improved performance should be traced to low levels of interstitial (or substitutional) nitrogen rather than to good NbN phases. Same results were found for samples that were cutout of N doped cavities with very high Q.

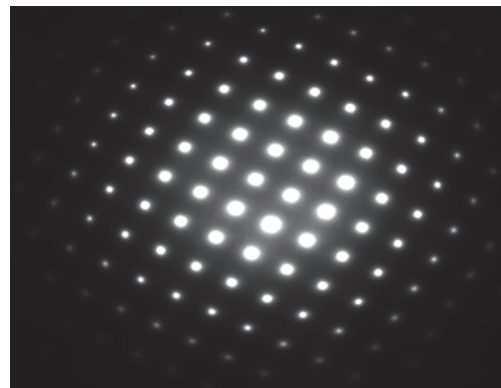


Figure 5: Diffraction pattern of transmitted electrons through a nitrogen baked plus EP sample, showing only clean Nb lattice (no nitride phases).

Once it was established that low levels of nitrogen in the niobium lattice were the origin of the improved performance, we investigated samples with SIMS, in particular we studied samples treated with cavities baked with different recipes and undoped samples as a comparison. Figure 6 shows a comparison among different samples for the nitrogen concentration as a function of depth. The doped samples have a nitrogen concentration $\sim 10-50$ times larger than the undoped

samples. This corresponds to a nitrogen concentration in the range 50-200 ppm. In the next paragraph we will describe how this concentration seems to affect R_{BCS} , R_0 , quench field and sensitivity to trapped magnetic field.

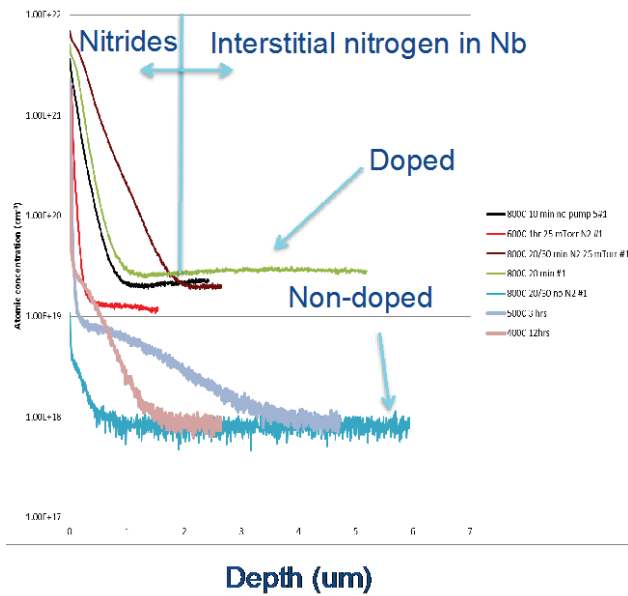


Figure 6: SIMS analysis for samples doped with different recipes versus undoped samples.

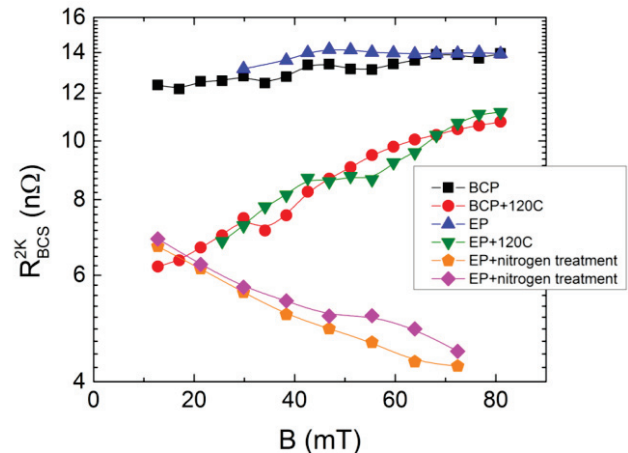


Figure 7: R_{BCS} as a function of the accelerating field for two doped, two 120C baked and two EP/BCP cavities, showing the origin of the peculiar “anti-Q-slope” in doped cavities.

One of the peculiarities of the N doped cavities is the absence of medium field Q-slope, or actually the reversal of the typical field dependence of the surface resistance in the mid field regime. The extended Q rise with the accelerating field has already been shown via surface resistance decomposition studies [8] to arise from the inverse field dependence of the BCS surface resistance [1,9], which, as shown in Fig. 7, decreases for N doped cavities but increases for 120C bake cavities with the

accelerating field. Several experiments at FNAL and other labs [10,11] and theoretical investigations [12,13] exist, that have brought new insights and explained the origin of this inverse field dependence. One interesting recent finding at FNAL comes from low energy muSR measurements performed at PSI [14,15]. Two cutout samples from a 120C bake cavity and from a N doped cavity (with high Q antislope performance) were studied with LEM and it was found that the penetration depth has a field dependence which increases with field for the 120C bake case and decreases with field for the N doping case. This can be seen in the results summarized in Fig. 8. The field dependence of the penetration depth has been measured before for type 2 superconductors, and could explain why the BCS surface resistance increases with field in one case and decreases in the other.

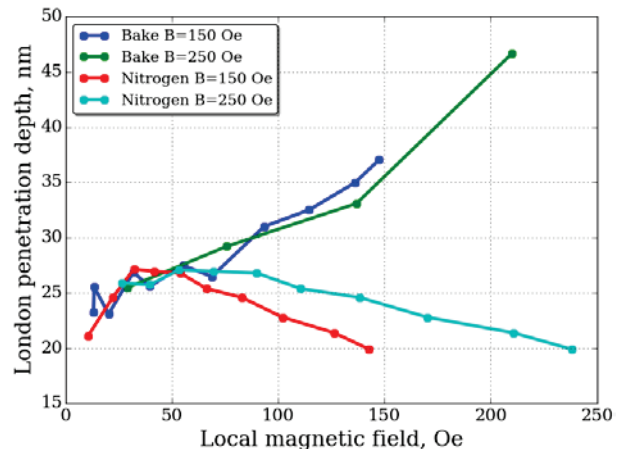


Figure 8: London penetration depth measured via LEM muSR for 120C baked and N doped cut-out samples as a function of applied parallel field.

Figure 9 shows the comparison of the low field measurements of the penetration depth via low energy muSR for 120C bake, EP/BCP [14] and N doped cavity cutout samples. It is interesting to notice that the standard treatments create a surface mean free path systematically in the very dirty (<10 nm, 120C bake) and very clean (>400 nm, EP/BCP) limits, while the N doping brings the surface to an intermediate mean free path range. These observations were confirmed by measurements conducted at FNAL [15] and Cornell [16] on cavities doped with different recipes, which produced different nitrogen concentration levels corresponding to mean free paths range 40-200 nm. Figure 10 shows the measurements of the 2K BCS surface resistance of 1.3 GHz cavities 120C baked, doped (different mean free paths) and EP/BCP at 5 and 16 MV/m accelerating fields. The low field BCS fit is shown as a comparison for two values of gap ~ 1.85 and $\sim 2 K_B T_c$. The latest stronger gap value, which is typically measured for N doped surfaces, brings the fit closest to the experimental values. It seems that the experimental data could be brought together via a combination of different mean free paths and different field dependences of the gap for the different surfaces, or different field dependences of the penetration depths (which acts on the

BCS pre-factor), which would be consistent with the measurements shown in Fig. 8. More detailed analyses to disentangle and pinpoint the origin of the BCS field dependence will be subject of future studies.

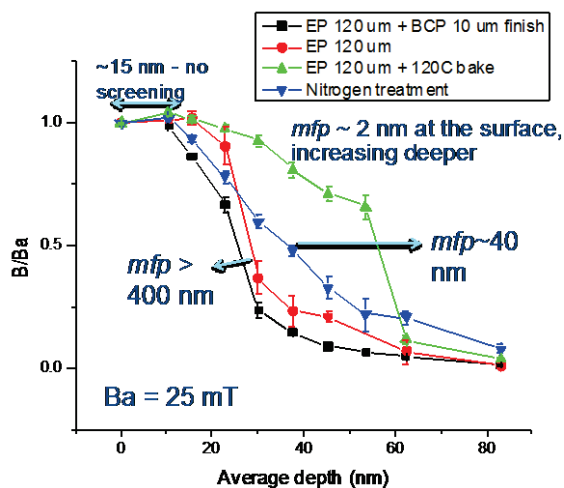


Figure 9: London penetration depth measured via LEM muSR for 120C baked, EP/BCP and N doped samples.

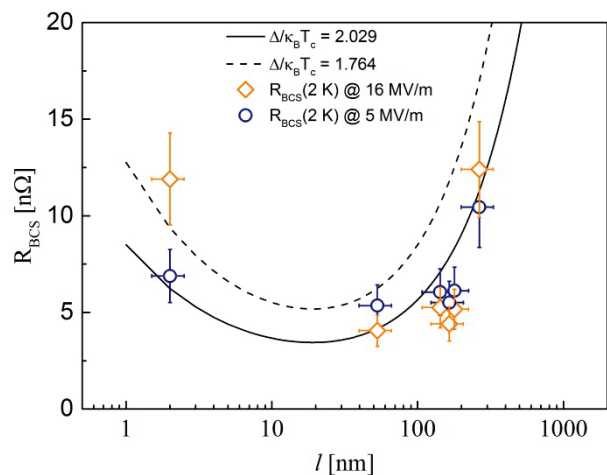


Figure 10: Experimental versus model of R_{BCS} resistance as a function of mean free path for doped and non-doped cavities.

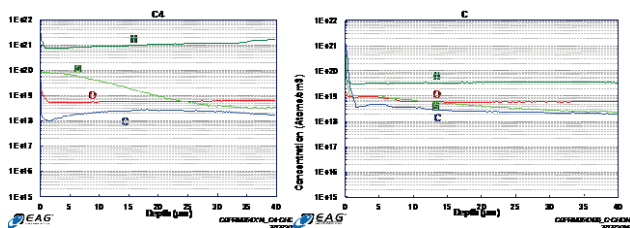


Figure 11: SIMS analysis for two samples treated with “heavy” and “light” doping respectively.

OPTIMAL RECIPE DEVELOPMENT

It has been previously reported [17,18] that there is a window of nitrogen surface concentration that leads to near optimal performance in terms of Q and quench fields. Below and above this window of concentration,

which is currently roughly estimated as 50-200 ppm from SIMS measurements, the cavity enters the so called overdoped versus underdoped regimes, whose effects on RF performance is described in the upcoming paragraph. Figure 11 shows two examples of doped samples whose nitrogen concentration, studied via SIMS, spans the overdoped to under doped regimes. In this contribution we also add the finding that the nitrogen level strongly affects the RF losses per trapped flux, which becomes one more variable contributing to the optimization of the doping recipe.

Optimal versus Overdoped/Underdoped Regimes

To explain the difference between optimal and non-optimal doping regimes, we now summarize how the different surface resistance components and quench fields are affected by different doping levels. The observations that follow are summarized in the Q curves and breakdown in residual and BCS shown in Fig. 12.

- R_{BCS} (Bpk > 60 mT)
 - This is the most robust parameter; R_{BCS} is systematically low for a very wide range of N concentration at the surface (> ~ 50 ppm); the optimal R_{BCS} (1.3 GHz, 2 K, >60 mT) is found to be 4.5 nΩ, < half of that of standard treatments (EP/BCP, 120C bake).
 - Below this concentration the surface enters the underdoped regime, with the R_{BCS} gradually returning to that of standard treatments (>8 nΩ).
- R_{BCS} (Bpk > 60 mT)
 - This is the most robust parameter; R_{BCS} is systematically low for a very wide range of N concentration at the surface (> ~ 50 ppm); the optimal R_{BCS} (1.3 GHz, 2K, >60 mT) is found to be 4.5 nΩ, < half of that of standard treatments (EP/BCP, 120C bake).
 - Below this concentration the surface enters the underdoped regime, with the R_{BCS} gradually returning to that of standard treatments (>8 nΩ).
- R_0 (non-trapped flux related)
 - If “overdoped” (> ~ 200 ppm) a strong field dependence of the surface resistance appears, with the onset being pushed higher with more subsequent material removal (lowering of the concentration).
 - Ideal concentration gives a ‘flat’ residual resistance systematically < 1.5 nΩ.
 - If “underdoped”, residual continues to stay low for a much wider range than R_{BCS} .
- Sensitivity to trapped magnetic flux
 - Lower doping levels (larger mean free paths) lead to smaller losses per trapped flux [15], with coefficient ranging from as high as 2 nΩ/mG to lowest found so far as 0.9 nΩ/mG.
- Maximum quench field
 - If overdoped quench <20 MV/m typically, worsening with higher doping levels.

- Quench fields improve with lighter doping, as it will be described in detail in the next paragraph, best quench fields reached are ~ 31 MV/m at FNAL, 35 MV/m at Cornell [19] and 39 MV/m at Jlab [20] for single cells. For nine cells best doping recipe at FNAL produces ~ 29 MV/m.

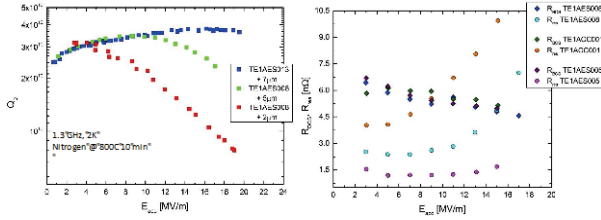


Figure 12: Examples of Q curves and R_{BCS} and R_0 for cavities overdoped and near optimal doping.

Quench Fields in N Doped Cavities

Interestingly, N doping affects strongly quench fields, which are typically lower in N doped cavities than for standardly treated ones. Quench fields are found to ‘cluster’ around a value dictated by the surface concentration. This is clearly seen in Fig. 13, for the nine cell cavities treated with two different recipes one leading to light doping levels (2/6 + 5EP) and one to heavy doping levels (20/30 + 15EP). While Q is very high for both cases, the quench fields are clearly centered around two different values 17 MV/m and 23 MV/m. The observation of the systematic lower quench fields clustered around a value depending on the doping level is consistent with magnetization measurements conducted on samples of different doping levels [21]. These measurements shown in Fig. 14 find that the field of first flux penetration is lowered with increasing doping levels.

The optimal doping recipe for quench field is yet under active research. The best recipes so far produce ~ 30 MV/m on single cells and ~ 28 MV/m on nine cells. It is interesting to notice that from single cell to nine cell there is a reduction of quench fields typically observed for same recipe used. This may be consistent with either EP being less homogenous for a nine cell surface and therefore having a higher probability that the cavity will see higher doping levels in certain cavity areas, or to more probability of having surface defects which coupling with lower field of first flux entry would yield to lower quench fields. Another speculative explanation for early quench in N doped cavities could be that residual nitrides may still persist even post electro-polishing. Figure 15 shows (bottom) an example of nitrides large and sharp protrusions, which may grow preferentially along some directions and perhaps leave residual poor SC phases of nanonitrides post EP. Top of Fig. 15 shows SEM images of two samples baked with nitrogen both for 20 minutes, but one without post nitrogen injection annealing and one with 30 minutes annealing at 800C. The two steps diffusion sample shows significant nitride growth compared to the first one. In nine cells, a trend has been seen where two-step anneal cavities quench earlier with

longer annealing times. These findings are summarized in Table 1.

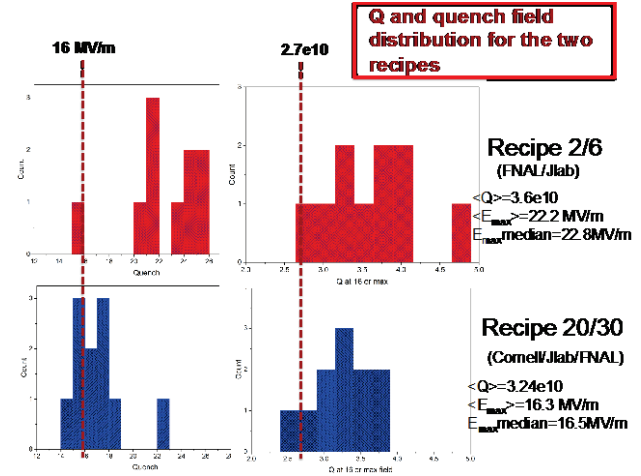


Figure 13: Statistics for Q and quench fields for 20 1.3 GHz nine cell cavities treated with light and heavy doping.

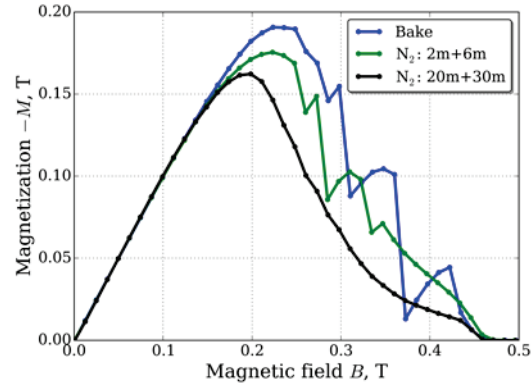


Figure 14: Magnetization measurements for 120C bake and N doped samples [21].

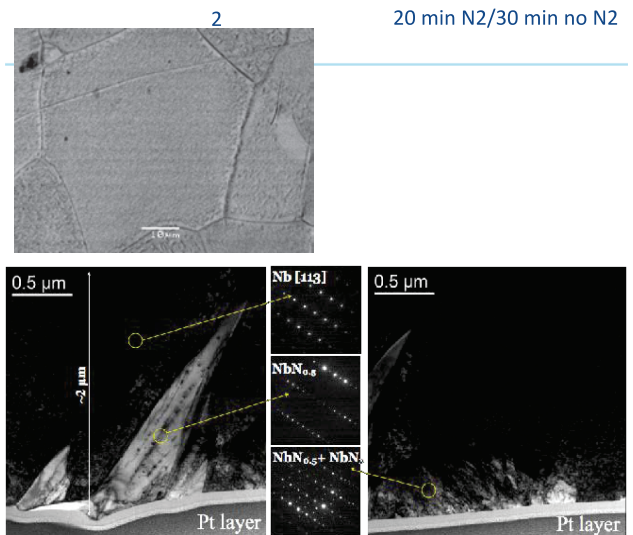


Figure 15: (top) SEM images of nitride formation on N treated samples; (bottom) sample cross section showing sharp nitrides penetrating the surface.

Table 1: Summary of Quench Fields for Cavities Doped with Different Recipes

Cavity ID #	Doping recipe [injection anneal minutes]	EP [microns]	Quench field [MV/m]
TB9ACC014	20	5	26
TB9ACC014	20	10	25
TB9ACC014	2/6	5	22
TB9ACC014	2/30	5	17
TB9ACC014	2/30	10	19
TB9AES022	2/0	5	26
TE5CAT006	10/60	5	12
TB9AES028	2/6	5	24
TB9AES028	2/6	8	28.5

Quench in N doped cavities has been studied at FNAL with temperature mapping [22]. Results of these studies suggest that the origin of the quench is magnetic rather than thermal, as the quench is sudden and with no pre-heating. Multipacting has been a suspected culprit of the premature quenches in N doped cavities, since often these quenches come at field levels compatible with being in a multipacting band, and sometimes accompanied by x-rays. However the studies in [22] seem to rule out MP as possible cause of quench.

Trapped Flux Losses and Optimal Point R_{BCS} - R_{FL}

It has been reported previously [23,24] that N doped cavities have a higher sensitivity to magnetic field than standardly treated ones. Recent experimental progress [15,25] has shown that this sensitivity strongly depends on the doping recipe used and that for lighter doping in reality it is not much higher than for standardly treated cavities. It is important to first remark that two very distinct factors play a separate role in how much cavity performance is affected by trapped magnetic flux:

- How efficiently the cavity de-traps flux
- How much the cavity surface dissipates per unit of trapped flux

Recent experimental progress has demonstrated that:

- N doped cavities do not trap more magnetic flux than standardly treated ones, so efficiency of flux de-trapping is only affected by bulk properties, not by doping or other surface treatments [26]
- N doped surfaces can dissipate more per unit of trapped flux. This is because trapped flux converts onto losses via mean free path and normal state resistivity, and that is a strong function of the doping recipe [15].

- Losses per trapped flux depend also on the accelerating field level, and the field dependence is stronger for non-doped cavities; this means that if compared at mid-higher fields N doped cavities are only slightly more sensitive compared to regular cavities, see Table 2 for reference values [15].

Table 2: Summary of RF losses factors per trapped magnetic flux for different surface processing

Surface processing	Residual Losses per trapped flux [nΩ/mGauss] @ 16 MV/m
120C bake	0.5
EP/BCP	0.7
2/6 doping + 5EP	1.24
2/6 doping + 8EP	0.9
10 min doping + 5EP	1.24
20 min doping + 5EP	2

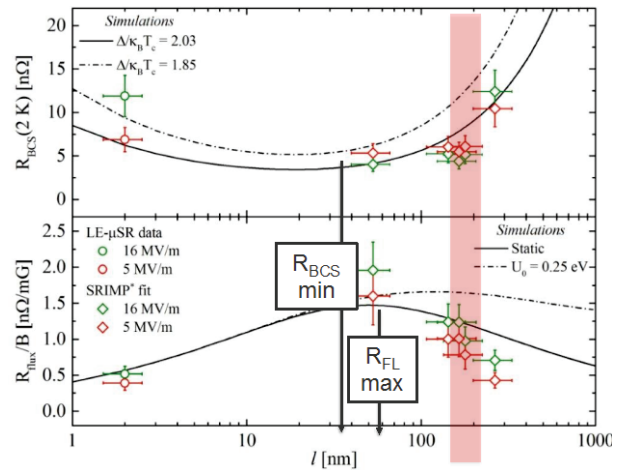


Figure 16: R_{BCS} and trapped flux induced resistance as a function of mean free path for cavities doped and non-doped. Experimental data is shown versus models.

Summarizing all these findings, the optimal doping recipe comes for lighter doping levels, which tremendously benefit quench fields and trapped flux losses. The ideal point to be found is the one that maximizes quench and minimizes trapped flux losses while maintaining minimum BCS surface resistance. Figure 16 shows BCS and trapped flux induced losses as a function of mean free path. The experimental data show that even though the minimum of R_{BCS} corresponds closely to the maximum of trapped flux induced residual resistance, there is a good range of mean free paths for which R_{BCS} is still at minimum value ~ 4.5 nΩ, while the trapped flux losses drop to less than 1 nΩ/mGauss and quench fields >22 MV/m. This range of larger mean free paths for N doped cavities is not yet fully explored and

therefore the optimal doping recipe is still under active research and studies.

CONCLUSIONS

Large progress has occurred in the past two years on nitrogen doping processing development and in the understanding of the root of the improved performance thanks to samples surface studies. Following rapid development, the technology is now ready for being used in the LCLS-2 accelerator with the potential to cut the cryogenic losses of this machine by a factor of two. The understanding of the underlying phenomena leading to the higher quality factors is being pursued theoretically and experimentally, and research towards an optimal doping treatment – which would give high Q at even higher fields (>25 MV/m) is ongoing.

ACKNOWLEDGMENT

This work was supported by the US Department of Energy, Offices of High Energy and Nuclear Physics, and via the LCLS-II project. Authors would like to acknowledge technical assistance of A. Rowe, B. Golden, D. Bice, B. Stone, C. Thompson, A. Diaz, J. Rife, D. Burk, B. Squires, G. Kirschbaum, D. Marks, and R. Ward for cavity preparation and testing. Fermilab is operated by Fermi Research Alliance, LLC under Contract No. DE-AC02-07CH11359 with the United States Department of Energy.

REFERENCES

- [1] A. Grassellino et al., *Supercond. Sci. Technol.* 26 (2013) 102001 (6pp)
- [2] A. Crawford et al., "The Joint High Q0 R&D Program for LCLS-II," in *International Particle Accelerator Conference 2014*, Dresden, Germany, (2014), p. 2627.
- [3] P. Bishop et al., MOPB033, in *SRF15 17th International Conference on RF Superconductivity*, Whistler, Canada (2015).
- [4] Y. Trenikhina, MOPB055, in *SRF15 17th International Conference on RF Superconductivity*, Whistler, Canada (2015).
- [5] J. Galayda et al., in *27th Linear Accelerator Conference*, Geneva, Switzerland, (2014), p. 404.
- [6] P. Derwent, S. Holmes, V. Lebedev, arXiv:1502.01728.
- [7] M. Checchin, INFN-SSSA Summer Internship Final Report, Fermilab, USA (2013).
- [8] A. Romanenko, A. Grassellino, *Appl. Phys. Lett.* 102, 252603 (2013).
- [9] D. Gonnella et al., "Performance of a FNAL Nitrogen Treated Superconducting Niobium Cavity at Cornell" *Proceedings of SRF13*, Paris, France (2013).
- [10] A. D. Palczewski et al., in *27th Linear Accelerator Conference*, Geneva, Switzerland, (2014).
- [11] D. Gonnella et al., in *27th Linear Accelerator Conference*, Geneva, Switzerland, (2014), p. 84.
- [12] A. Gurevich, *PRL*, 2014. 113(8): p. 087001.
- [13] B.P. Xiao et al., *Physica C: Superconductivity* (2013) 490(0): p. 26-31
- [14] A. Romanenko et al., *Appl. Phys. Lett.* 104, 072601 (2014).
- [15] M. Martinello et al., MOPB015, in *SRF15 17th International Conference on RF Superconductivity*, Whistler, Canada (2015).
- [16] D. Gonnella et al., "Sensitivity of Niobium Superconducting RF Cavities to Magnetic Field," in *SRF 17th International Conference on RF Superconductivity*, Whistler, Canada (2015).
- [17] A. Grassellino, TUIOA03, "New Insights on the Physics of RF Surface Resistance and a Cure for the Medium Field Q-Slope", in *16th International Conference on RF Superconductivity*, Paris, France (2013).
- [18] A. Grassellino, "N-doping Process - Physics and Technique," LCLSII-4.5-EN-0218-R0, SLAC (2014).
- [19] D. Gonnella et al., "Nitrogen-Treated Cavity Testing at Cornell", *Proceedings of LINAC14*, Geneva, Switzerland (2014).
- [20] R. Geng, WEPWI013, in *Proceedings of IPAC 2015*, Richmond, Virginia.
- [21] A. Vostrikov et al., MPOB027, in *SRF15 17th International Conference on RF Superconductivity*, Whistler, Canada (2015).
- [22] M. Checchin et al., WEPTY034, "T-map Studies on Gradient-limiting Mechanism in Nitrogen Doped Cavities", in *Proceedings of IPAC 2015*, Richmond, Virginia.
- [23] A. Romanenko et al., "Dependence of the residual surface resistance of SRF cavities on the cooling rate through Tc," *J. Appl. Phys.*, 115(184903), (2014).
- [24] D. Gonnella et al., in *6th International Particle Accelerator Conference*, Richmond, VA (2015), p. 3446.
- [25] M. Checchin et al., "Mean Free Path Dependence of the Trapped Flux Surface Resistance", MOPB020, in *SRF15 17th International Conference on RF Superconductivity*, Whistler, Canada (2015).
- [26] S. Posen, "Flux Expulsion Variation in SRF Cavities", MOPB104, in *SRF15 17th International Conference on RF Superconductivity*, Whistler, Canada (2015).